Available online at www.sciencedirect.com
SCIENCE DIRECT®
Chemical Physics 292 (2003) 487–494
Chemical Physics
www.elsevier.com/locate/chemphys

TOF-elastic resolution spectroscopy: time domain analysis of weakly scattering (biological) samples

W. Doster[a,*], M. Diehl[a], R. Gebhardt[a], R.E. Lechner[b], J. Pieper[b]

[a] *Physik Department E 13, Technische Universität München, D-85748 Garching, Germany*
[b] *Hahn-Meitner Institut (BENSC), Berlin, Germany*

Received 2 December 2002; in final form 24 March 2003

Abstract

Elastic resolution spectroscopy (ERS), a new application of the time-of-flight method, addresses the problem of weak scattering signals. Since only the maximum of the spectrum at zero energy transfer needs to be determined with sufficient statistical accuracy, significantly smaller samples, as compared to conventional spectroscopy, can be studied. The peak intensity is recorded versus the reciprocal width of the instrumental resolution function by adjusting the speed of the chopper system. This approach yields a close approximation to the intermediate scattering function in the time domain. A neutron ERS analysis of molecular motions in alanine-dipeptide crystals and hydrated myoglobin is presented.

1. Introduction

One of the main limitations of neutron spectroscopy is the requirement of large samples. Because of the low luminosity of available neutron sources and the small scattering cross-section of neutrons, even of hydrogenated systems, long beam times are necessary. For dynamic studies of proteins, typically 200–400 mg of material have to be exposed to the beam for 6 h to collect sufficient neutrons in the wings of the spectrum [1,2]. This restriction excludes most of the interesting systems of molecular biology, where more than a few milligrams are rarely available. Furthermore, the new prospects of labelling proteins, using partial or full deuteration, will further reduce the cross-section, implying that even more material is needed. We have shown recently, that 23 mg of protein can be sufficient to determine the maximum intensity of the spectrum and subsequently its intermediate scattering function [3]. A second class of applications concerns protein solutions, where the polymer component can be discriminated from the intense coherent background of the solvent because of a narrow elastic peak [4]. Often in biological applications one is interested in observing small dynamic changes in response to some external perturbation. Fig. 1 shows the neutron scattering spectra of bacteriorhodopsin, a protein, which forms a hexagonal lattice in purple

* Corresponding author. Tel.: +49-89-289-12456.
E-mail address: wdoster@ph.tum.de (W. Doster).

0301-0104/03/$ - see front matter © 2003 Elsevier Science B.V. All rights reserved.
doi:10.1016/S0301-0104(03)00156-3

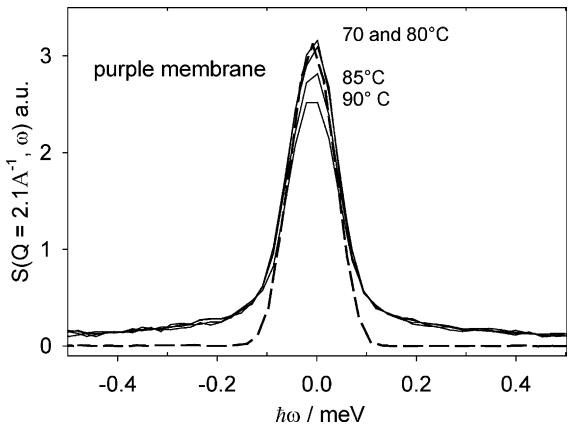

Fig. 1. Bacteriorhodopsin at the melting transition of its hexagonal lattice measured with the TOF spectrometer V3 at the HMI in Berlin [6]. Dashed line: resolution function (Vanadium).

membranes. The temperature sequence displays the effect of melting of the lattice on protein-internal motions [5,6]. A decrease in elastic intensity is clearly visible in the central region of the spectrum. The increase in translational degrees of freedom leads to a lower elastic intensity. According to the sum rule, the "lost" intensity appears in the broad wings of the spectrum, which is, however, difficult to detect. To discriminate the different curves with sufficient statistical accuracy from each other in the wings of the spectrum requires much longer runtimes.

The same information can be obtained by recording the maximum intensity at variable instrumental resolution. The main objective of elastic resolution spectroscopy is to derive the relevant dynamic information from the easy to detect maximum of the spectrum without resorting to the wings. The central idea is to introduce the time axis via the energy resolution function of the instrument.

If the primary spectrometer could select a sharp wavelength, λ_0, an infinite plane neutron wave without time limitation would result. Instead, a narrow distribution of wavelengths of width $\Delta\lambda$ is selected, which leads to a finite coherence length. The finite length of the neutron wave packet, which moves with average velocity $v = h/(m_N\lambda_0)$ across the scattering centres, limits the scattering time to $t \leqslant \hbar/\Delta E_0 = m_N\lambda_0^3/(h\Delta\lambda)$. "$m_N$" is the neutron mass and ΔE_0 denotes the width of the initial energy distribution. Choosing $\lambda_0 = 5.1$ Å and $\Delta\lambda = 0.1$ Å, yields a time window of 33 ps. By varying λ_0 and $\Delta\lambda$ or E_0 and ΔE (resolution), one is scanning the time window of observation [3,7]. Technically this can be achieved with existing TOF–TOF spectrometers, IN5 [8,9], MIBEMOL [10], NEAT [11–13], built specifically with this option. The change of the time window is obtained by varying one or several of the following parameters, the incident neutron-wavelength, the speed of the chopper system, the chopper-window width, or one of the flight distances. It is shown below that the maximum intensity, recorded as a function of the reciprocal energy resolution, approximates the scattering function $I(Q,t)$ in the time domain. The elastic intensity and the intermediate scattering function are related to the probability that an average atom is residing for a selected time interval t inside a space interval $x = 2\pi/Q$. ERS thus extends the well-known fixed-window method, where dynamic information is derived from "elastic scans" versus temperature at fixed energy resolution [1,14,15].

2. Theoretical background

With inelastic neutron scattering one intends to determine the dynamical structure factor $S(Q,\omega)$ or its Fourier-transform, the intermediate scattering function $I(Q,t)$ [8]. Instead, the experimentally accessible quantity is the scattering function $S_R(Q,\omega,\Delta\omega)$, which is given by the convolution of the dynamic structure factor $S(Q,\omega)$ with the resolution function of the instrument $R(\omega,\Delta\omega)$

$$S_R(Q,\omega,\Delta\omega) = \int_{-\infty}^{\infty} R(\omega-\omega',\Delta\omega)\,S(Q,\omega')\,d\omega'. \tag{1}$$

The scattering function $S_R(Q,\omega,\Delta\omega)$ can be interpreted as the dynamic structure factor with respect to a fixed observation time window $t = 1/\Delta\omega$, the reciprocal width of the energy resolution function. A related quantity is the peak intensity at zero nominal energy transfer of Eq. (1), which is given by

$$P(Q,t=1/\Delta\omega) \propto S_{\mathrm{R}}(Q,\omega=0,\Delta\omega) = \int_{-\infty}^{\infty} R(\omega',\Delta\omega)\, S(Q,\omega')\,\mathrm{d}\omega'. \quad (2)$$

The goal is to derive, based on Eq. (2), an approximation to the intermediate scattering function $I(Q,t)$, the Fourier transform of $S(Q,\omega)$

$$I(Q,t) = \int_{-\infty}^{\infty} \cos(\omega' t)\, S(Q,\omega')\,\mathrm{d}\omega'. \quad (3)$$

Note that Eq. (2) has the structure of a frequency-time transform like Eq. (3), provided that we set $t = 1/\Delta\omega$. An exact identity obtains if $R(\omega,t)$ is replaced by the kernel of the Fourier integral "$\cos(\omega t)$". This situation is approximately realised within the framework of spin-echo spectroscopy (NSE) [16]. The configuration of the spectrometer is such, that an effective inverse resolution is defined, the so-called spin-echo time τ_{SE}. The equivalent quantity to the elastic intensity is the residual polarisation, $P_{\|}(Q,\tau_{\mathrm{SE}})$, which is measured as a function of the resolution parameter. The precession of the neutron spins in the magnetic field serves as a clock to determine the flight time of the neutrons. Changing the strength of the magnetic field modifies the precession frequency and thus with $\tau_{\mathrm{SE}}(H)$ the sensitivity of the configuration to small velocity differences induced in the sample.

In contrast to NSE, the resolution function of a TOF spectrometer exhibits approximately a Gaussian line-shape, because of the convolution of several triangular width functions of the individual choppers and path length variations with statistical distribution. The Gaussian shape is a good approximation for both, the time and energy domain of the spectrum, provided that the resolution function is reasonably narrow. Assuming a Gaussian line-shape $G(\omega,\sigma) = \exp(-\omega^2/2\sigma^2)$, we write instead of Eq. (3)

$$P_\sigma(Q) = \int_{-\infty}^{\infty} \exp\left(-\frac{\omega^2}{2\sigma^2}\right) S(Q,\omega)\,\mathrm{d}\omega, \quad (4)$$

which is the Gauss (–Laplace) transform of the dynamical structure factor. σ denotes the standard deviation. For the generic case of a Lorentzian spectrum, $S(Q,\omega,\tau) = (1/\pi)\,\tau/(1+\omega^2\tau^2)$ which corresponds to an exponential correlation function with correlation time τ, a closed form is obtained

$$P_\sigma(Q,\tau) = f(Q)\, erfc\left(\frac{1}{\sqrt{2}\sigma\tau}\right) \exp\left(\frac{1}{2\sigma^2\tau^2}\right), \quad (5)$$

where $f(Q)$ schematically accounts for the dependence of the spectrum on Q. Eq. (5) enables one to extract the relevant dynamical information from the ERS data as discussed in [3]. $erfc(x)$ is the complementary error function. Since $erfc(x)\cdot\exp(x^2) \approx \exp(-x)$ for $x \ll 1$, an exact short time expansion of the FT of $S(Q,\omega,\tau)$ is obtained, if we choose: $t = 1/(\sqrt{2}\cdot\sigma)$.

For practical purposes we introduce the FWHM in energy space: $\Delta E_{\mathrm{G}} = 2\hbar\sigma\sqrt{(2\ln 2)}$. The time scale in terms of the FWHM (meV) in picoseconds is then given by: $t = 1.09/\Delta E_{\mathrm{G}}$ (meV) ps. Fig. 2 compares the exact $I(Q,t)$, an exponential correlation function, full line, with the ERS result of Eq. (5) (dashed-dotted).

The ERS approximation to the Fourier transform of $S(Q,\omega)$ is excellent only at short times. The long time tail of the ERS-function (Eq. (5)) is related to contribution at $\omega = 0$ of the fully resolved Lorentzian spectrum for small σ or large t. One obtains an algebraic decay of $P_\sigma(t\to\infty) = \sqrt{2/\pi}\cdot\tau/t$, while the correlation function $I(t)$ is vanishing exponentially [3].

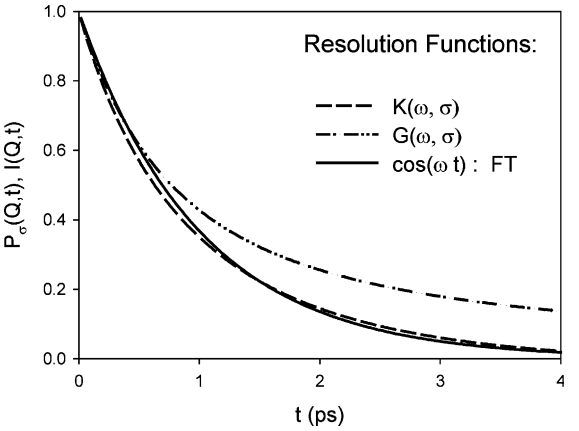

Fig. 2. The integral transforms of a Lorentzian, $S(\omega,\tau=1\text{ ps})$, using different kernels: (1) FT: $\cos(\omega t)$: $I(Q,t)$; (2) Gaussian $G(\omega,\sigma)$, Eq. (5); and (3) a combination of three shifted Gaussians: $K(\omega,\sigma)$, Eq. (6).

3. Results

3.1. A Fourier-like ERS kernel

The Gauss–Laplace transform of the dynamical structure factor contains the same amount of information as its Fourier transform. Only Eq. (5) replaces the exponential time decay. A sum of such expressions is required to describe multi-component systems [3]. Since, however, Fourier transforms are so well established, we look for an improved ERS approximation to the intermediate scattering function $I(Q,t)$. For this purpose the Gauss kernel $G(\omega,\sigma)$ is replaced by a symmetric combination of three frequency-shifted Gauss functions $K(\omega,\sigma)$

$$K(\omega,\sigma) = G(\omega,\sigma) - \frac{1}{2}G(\omega-\pi\sigma,\sigma) - \frac{1}{2}G(\omega+\pi\sigma,\sigma). \quad (6)$$

This kernel is compared in Fig. 3 with the Fourier kernel. The resulting elastic intensity function $P_\sigma(Q,t)$, displayed in Fig. 2, improves the approximation to the true intermediate scattering function in particular at long times as compared to a Gauss kernel. For this correction one subtracts from the experimental peak intensity at $\omega = 0, 1/2$ of the "inelastic" intensities at $\omega \approx \pm\pi\sigma$.

3.2. Experimental considerations

For practical applications of ERS, the peak intensities $P_\sigma(Q)$ covering a wide range of instrumental resolutions σ have to be determined. Existing time-of-flight (TOF–TOF) spectrometers, for instance NEAT, allow the scanning of the chopper speed from 1000 to 20,000 rpm. The width of the energy resolution is roughly proportional to reciprocal chopper speed. A wider range is achieved by varying in addition the incoming wavelength λ_0 since approximately: $\Delta E \propto 1/\lambda_0^3$. A time window ranging from 0.5 ps up to almost nanoseconds is feasible. An example is discussed below. In continuous beam TOF–TOF spectrometers (IN5, NEAT, MIBEMOL) both, the wavelength selection and the choice of the energy resolution are achieved by chopper systems. It is thus easy to implement the ERS technique as a standard user. The TOF spectrometer basically registers the detected neutrons in a set of channels n, equally spaced in time with intervals Δt, versus their respective time of flight $t_f = n \cdot \Delta t$. The elastic flight time is t_0. With proper normalisation to the incident flux, the area and the sensitivity of the detectors, the number of neutrons registered at the maximum intensity is given by

$$P(Q,t_0) = \Delta t \int \mathrm{d}t_f R'(t_f,t_0)\frac{\partial^2\sigma(\Omega,t_f)}{\partial\Omega\partial t_f}. \quad (7)$$

The peak function $P(Q,t_0)$ is the main object of an ERS measurement. $R'(t_f,t_0)$ denotes the normalised instrumental resolution function at the elastic flight time t_0.

The double differential cross-section is related to the dynamical structure factor $S(Q,\omega)$ via a time-frequency transformation [21]:

$$\frac{\partial^2\sigma}{\partial\Omega\partial t} = \left|\frac{\mathrm{d}\omega}{\mathrm{d}t_f}\right| N\frac{k(t_f)}{k_0}S(Q(t_f),\omega(t_f)), \quad (8)$$

where N represents the total scattering power of the sample. k_0 and $k(t_f)$ are the incident and the final wavevectors, respectively. Since their magnitude does not change at the elastic peak and since the width of $R(t_0)$ is usually small compared to t_0, we can write: $k(t_f) \approx k(t_0) \approx k_0$ and $Q(t_f) = Q_{\mathrm{elas}} = Q$. We thus approximate Eq. (7) by

$$P(Q,t_0) = N\Delta t \int \mathrm{d}\omega R'(t_0,t_f(\omega))S(Q,\omega). \quad (9)$$

Assuming a Gaussian resolution function appropriate for TOF spectrometers

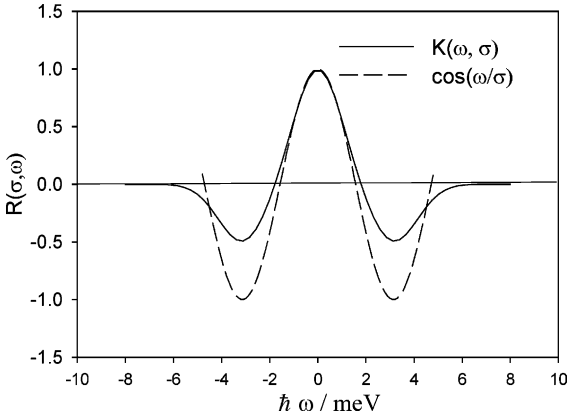

Fig. 3. FT kernel $\cos(\omega/\sigma)$ in comparison with $K(\hbar\sigma = 1\ \mathrm{meV})$ of Eq. (6).

$$R_\sigma(\omega) = \frac{1}{\sqrt{2\pi}\sigma} \exp\left(-\frac{\omega^2}{2\sigma^2}\right), \quad (10)$$

we obtain the at $t = 0$ normalised peak function

$$P_\sigma(Q,t) = \frac{P(Q,\sigma)\sqrt{2\pi}\sigma}{\Delta t N}, \quad (11)$$

which is the relevant quantity to be compared with the intermediate scattering function in Fig. 2.

Fig. 4 shows such a normalised Voigtian spectrum: a Lorentzian spectrum of width $\Gamma = 0.2$ meV has been convoluted with a Gaussian resolution function of variable width σ.

The σ-weighted peak intensity decreases with increasing resolution (decreasing σ), since the Lorenzian spectrum (dashed) becomes resolved. The smallest peak ($\hbar\sigma = 0.05$ meV) in Fig. 4 exhibits a limiting Lorentzian shape, the spectrum is fully resolved. The corresponding σ-weighted peak intensity P_σ is given by Eq. (5) in the long time limit $\propto \tau/t$.

3.3. Frequency and time domain TOF of alanine-dipeptide

To test the technical feasibility of ERS, we compare the time domain with the conventional frequency domain approach. For this purpose we investigated the molecular dynamics of 290 mg of alanine-dipeptide crystals (*N*-methyl-L-alanyl-*N*-methylamide: CH_3–CONH–$C_\alpha H(C_\beta H_3)$–CONH–CH_3).

This molecule is one of the simplest model peptides containing the basic fragments, necessary for a detailed understanding of the inter-atomic interactions present in proteins. We have characterised this system previously using conventional TOF neutron spectroscopy and MD simulation [17]. The N- and C-terminal methyl groups have low rotational barriers (3 kJ/mol) and perform diffusive motions on a picosecond time scale. The barrier for the side-chain methyl group is about 10.5 kJ/mol, leading to rotational jumps at 300 K. The respect rotational correlation functions should decay within 3 ps. Fig. 5 shows the ERS intermediate scattering function determined with the NEAT time-of-flight spectrometer at the Hahn-Meitner Institut in Berlin. The chopper speed was varied between 1000 and 10,000 rpm at three wavelengths: 5, 8 and 10 Å. The data at $Q = 2.3$ Å^{-1} were obtained using neutrons with an incident wavelength of 5 Å and by changing the chopper speed from 1000, 2000, 5000 to 10,000 rpm. Up to 20,000 rpm is possible. Runtimes were chosen such that about 2000 counts in the elastic peak per grouped spectrum were collected. Depending on

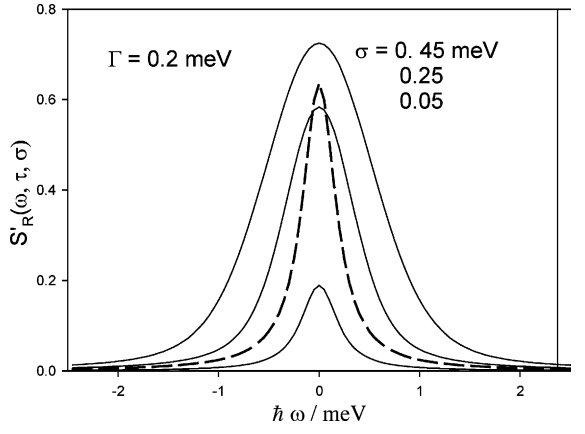

Fig. 4. Voigtian spectra, a Lorentzian function (dashed) of width $\Gamma = 0.2$ meV convoluted with a Gaussian resolution function of variable width. The σ-weighted peak intensity of this spectrum yields $P_\sigma(t)$: $S'_R(\omega = 0, \tau, \sigma) = \sqrt{(2\pi)}\,\sigma\, S_R(\omega = 0, \sigma) = P_\sigma(t)$ (Eq. (2)).

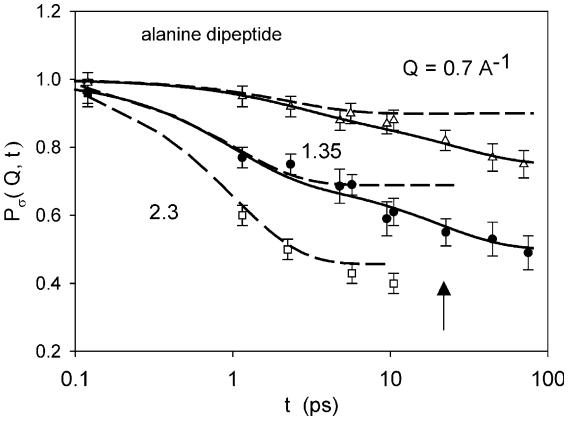

Fig. 5. ERS intermediate scattering function of alanine-dipeptide crystals at 300 K. The dashed lines represent the combined rotational correlation function of the three methyl groups. The full line includes an additional structural process with a correlation time of 20(±3) ps. The arrow indicates the time corresponding to the energy resolution of the spectrum shown in Fig. 6. NEAT spectrometer at BENSC.

chopper speed and wavelength, runtimes between 20 min and several hours were necessary. Channels containing extra intensity due to Bragg peaks of the crystal were excluded. Normalisation at short times was achieved using the count rates (corrected for detector efficiency) at low $Q = 0.2$ Å^{-1}. This approximation is consistent with the scattering law of the dipeptide, shown as dashed lines in Fig. 5. Measurements at lower wavelength (3.5 Å at 1000 rpm) would allow setting the initial time point to 0.3 ps. The ERS correlation function due to rotational motions of the three methyl groups in alanine-dipeptide decays rapidly at 300 K (Fig. 5), consistent with the conventional analysis in the frequency domain [17]. The ERS intermediate scattering function follows initially the predicted behaviour of rotational motions but decays further at long times.

A fit at $Q = 1.35$ Å^{-1} yields the correlation times, $\tau_1 = 1.5$ (± 0.5) ps for the rotational motion and $\tau_2 = 20$ (± 2) ps, suggesting a new structural process. Indications of the existence of a non-rotational process in alanine-dipeptide crystals have been obtained in our previous study. Its nature could not be identified since our MD simulations covered only 10 ps [17]. For direct comparison with ERS, a TOF spectrum was collected for 2 h at a particular chopper configuration of 5000 rpm and $\lambda = 8$ Å, corresponding to an observation time of 23 ps.

Fig. 6 shows the resulting scattering function at $Q = 1.35$ Å^{-1} on a log-scale together with a three component analysis: a Gaussian elastic spectrum and two Lorentzian quasi-elastic spectra specified by $\tau_1 = 1.5$ ps (dashed line), and $\tau_2 = 21$ (± 2) ps. The fitted curve in Fig. 6 (full line) is thus compatible with the time domain analysis of Fig. 5.

As the second example we discuss an experiment performed with a small sample, 23 mg of hydrated myoglobin, at the TOF spectrometer IN5 (old) in Grenoble [3]. Also a conventional analysis was performed with 300 mg of dry and hydrated myoglobin combining data measured with two different spectrometers: the time-of-flight spectrometer IN6 and of the back-scattering spectrometer IN10 at the ILL in Grenoble [18–20] (see Fig. 7). The two data sets agree reasonably well covering a time window of 1–450 ps. A two-exponential model including a long-time constant,

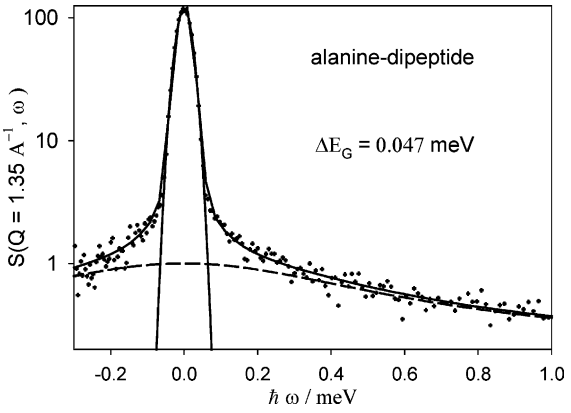

Fig. 6. Scattering function of alanine-dipeptide at $Q = 1.35$ Å^{-1} (dots) taken at $\lambda = 8$ Å and 5000 rpm (NEAT): $\Delta E_G = 0.047$ meV or 23 ps. The full line represents a fit to three spectral components observed in Fig. 5. The narrow Gaussian spectrum represents the ERS-fit to obtain the peak intensity. The broad spectrum (dashed) corresponds to the rotational motion of the methyl groups.

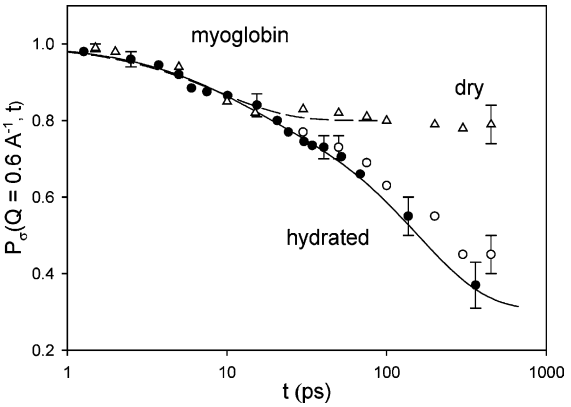

Fig. 7. ERS intermediate scattering function of 23 mg D_2O-hydrated myoglobin powder, full circles (IN5), and a two component fit (solid line). Open symbols: 300 mg of dry and hydrated myoglobin: Fourier-deconvoluted spectra of IN10 and IN6 (ILL Grenoble) at 300 K [3,18–20].

the elastic incoherent structure factor (EISF), is the minimum requirement to fit the data. The fast correlation time of $\tau_1 = 9$ (± 2) ps is related to dihedral transitions of side-chains and the main chain including the methyl group rotation [1]. The second time constant $\tau_2 = 150$ (± 30) ps is much longer and corresponds to liquid-like motions involving the hydration shell. For the asymptotic

value of $P_\sigma(Q, t \to \infty)$, the EISF ($Q = 0.6$ Å^{-1}), we derive 0.33 (± 0.03) in the hydrated case which involves some uncertainty due to the limited time window. Alternatively a stretched exponential provides a fit of similar quality. The decay of fast correlations in the dry system coincides with the hydrated case, but the slow component is missing [20]. The plateau value provides an estimate of the EISF(Q) of fast protein motions.

4. Conclusion

The ERS technique extends the potential of TOF-neutron spectroscopy to dynamic studies of weakly scattering samples. The effective transmission of the myoglobin sample was above 99%. Multiple scattering will be negligible with such samples. The dynamic information is obtained directly in the time domain, which avoids the necessity of Fourier deconvolution. In contrast to the conventional spin-echo technique there is no restriction concerning the nature of the scattering process, coherent or incoherent. Scanning the resolution within a wide range addresses the full potential of TOF spectrometers. ERS can be performed with existing spectrometers, no special equipment is involved. However, with weakly scattering samples more attention needs to be addressed to background scattering. Sample holders consisting of thin aluminium foils (10 μm) instead of the standard 0.2 mm aluminium cells should be used. Beam time considerations depend very much on the quality and quantity of the information requested. To measure the broad line in Fig. 6 (dashed) with similar statistical error as the central peak would involve factor of 100 in beam time at this configuration. Most standard fitting programs would treat the broad line as a disposable background (log scale!). With 300 mg of material one would probably measure spectra at two or three different instrumental resolutions, which would require slightly less than the 12 h used for this test ERS experiment. With 30 mg of material there would be little choice because of the low signal to noise in the wings of the spectra irrespective of the runtime. In practice one should combine both methods, since with ERS one is always collecting also spectral information. A particular advantage of the ERS method is that with most configurations the frame-overlap chopper can be run at ratio one, which increases the count-rate by a factor of two [3]. The IN5 experiment required about six days in beam time. This includes some low temperature experiments at 150 K, where the scattering is completely elastic, to check the normalisation at short times. With the upgrade of IN5, shorter exposure times are to be expected. In addition a new TOF–TOF spectrometer with similar properties is being installed at the new neutron source FRM II in Munich extending the ERS possibilities further.

Acknowledgements

The project is supported by a grant (DOE 2M1) of the Bundesministerium für Forschung und Technologie. Discussions with A. Desmedt and W. Petry are gratefully acknowledged.

References

[1] W. Doster, S. Cusack, W. Petry, Nature 337 (1989) 754.
[2] W. Doster, M. Settles, in: M.C. Bellissent-Funel, J. Teixera (Eds.), Hydration Processes in Biology, NATO Science Series A: Life Sciences, vol. 305, IOS Press, 1998, p. 177.
[3] W. Doster, M. Diehl, W. Petry, M. Ferrand, Physica B 301 (2001) 65.
[4] J. Perez, J.M. Zanotti, D. Durand, Biophys. J. 77 (1999) 454.
[5] J. Müller, C. Münster, T. Salditt, Biophys. J. 78 (2000) 3208.
[6] W. Doster, N.A. Dencher, Th. Hauß, R.E. Lechner, J. Pieper, 2003, to be published.
[7] R.E. Lechner, Physica B 301 (2001) 83.
[8] R.E. Lechner, F. Douchin, Y. Blanc, R. Scherm, Internal Reports of ILL Grenoble and KFA Jülich, 1973 (unpublished), see also (Chapter 3.2), in: M. Bée, Quasielastic Neutron Scattering, Adam Hilger, Bristol, 1988, pp. 81–85.
[9] R.E. Lechner, in: Neutron Scattering in the Nineties, IAEA, Vienna, 1985, p. 401.
[10] S. Hautecler, E. Legrand, L. Vansteelandt, P. d'Hooghe, G. Rooms, A. Seeger, W. Schalt, G. Gobert, in: Neutron Scattering in the Nineties, IAEA, Vienna, 1985, p. 211.
[11] R.E. Lechner, Physica B 180–181 (1992) 973.
[12] R.E. Lechner, R. Melzer, J. Fitter, Physica B 226 (1996) 86.

[13] B. Rufflé, J. Ollivier, S. Longeville, R.E. Lechner, Nucl. Instrum. Methods A 449 (2000) 322.
[14] B. Alefeld, A. Kollmar, B.A. Dasannachrya, J. Chem. Phys. 63 (1976) 4415.
[15] F. Fujara, W. Petry, Europhys. Lett. 4 (1987) 921.
[16] F. Mezei (Ed.), Neutron Spin Echo, Lecture Notes in Physics, Springer, Berlin, 1980; F. Mezei, C. Pappas, T. Gutberlet (Eds.), Neutron Spin Echo Spectroscopy, Lecture Notes in Physics, vol. 601, Springer, Berlin, 2003.
[17] G.R. Kneller, W. Doster, S. Cusack, M. Settles, J.C. Smith, J. Chem. Phys. 97 (1992) 8864.
[18] W. Doster, S. Cusack, W. Petry, Phys. Rev. Lett. 65 (1990) 1080.
[19] W. Doster, Modern Phys. Lett. B 5 (21) (1991) 1407.
[20] M. Diehl, W. Doster, W. Petry, H. Schober, Biophys. J. 73 (1997) 2726.
[21] M. Bee, Quasielastic Neutron Scattering, Adam Hilger, Bristol, 1988.